

Photochemistry

Deciphering Photoluminescence Dynamics and Reactivity of the Luminescent Metal–Metal-Bonded Excited State of a Binuclear Gold(I) Phosphine Complex Containing Open Coordination Sites

Chensheng Ma,^[a, d] Chris Tsz-Leung Chan,^[c] Wai-Pong To,^[a] Wai-Ming Kwok,^{*, [c]} and Chi-Ming Che^{*, [a, b]}

Abstract: Luminescent metal complexes having open coordination sites hold promise in the design of sensory materials and photocatalysts. As a prototype example, $[\text{Au}_2(\text{dcpm})_2]^{2+}$ (dcpm = bis(dicyclohexylphosphanyl)) is known for its intriguing environmental sensitive photoluminescence. By integrating a range of complementary ultrafast time-resolved spectroscopy to interrogate the excited state dynamics, this study uncovers that the events occurring in extremely rapid timescales and which are modulated strongly by environmental conditions play a pivotal role in the luminescence behavior and photochemical outcomes. Formed independent of the phase and solvent property within ~ 0.15 ps, the metal–metal bonded $^35d\sigma^*6p\sigma$ state is highly reactive possessing strong propensity toward increasing coordination number at Au^{I} center, and with ~ 510 ps lifetime in dichloromethane is able to mediate light induced C–X bond cleavage.

Luminescent Au^{I} complexes have garnered considerable interest for their fascinating photophysical properties and photochemistry.^[1–3] A family of dinuclear $d^{10}\text{–}d^{10}$ Au^{I} complexes containing bridging phosphine ligands, $[\text{Au}_2(\text{diphosphine})_2]^{2+}$, is of particular interest from the perspective of Au–Au bonding interactions^[1,2,4–6] and their intriguing photoluminescence,^[1,2,7,8]

all of which vary profoundly with factors such as nature of counter ion and solvent. The open coordination site of Au^{I} in $[\text{Au}_2(\text{diphosphine})_2]^{2+}$ is reminiscent of that of Pt^{II} in $[\text{Pt}_2(\text{P}_2\text{O}_5\text{H}_2)_4]^{4-}$ allowing the $^35d\sigma^*6p\sigma$ excited state to perform C–X activation and emissive exciplex formation at the inner coordination sphere.^[9,10] An outcome of these excited-state properties leads to micro-environmental dependence of luminescence on Au^I–Au^I interacting binuclear and polynuclear Au^I complexes, which has been used in the design of luminescence sensors and new materials for optoelectronic switches.^[4,6,11–14] More recently, $[\text{Au}_2(\text{diphosphine})_2]^{2+}$ has been reported as a new novel photocatalyst for light-induced organic transformation reactions.^[15,16]

An archetype example of $[\text{Au}_2(\text{diphosphine})_2]^{2+}$ is $[\text{Au}_2(\text{dcpm})_2]^{2+}$ (dcpm = bis(dicyclohexylphosphanyl)methane, **1**, Figure 1), a bi- Au^{I} complex bearing the UV-silent phosphine ligand.^[7] Irrespective of solvent properties (e.g. coordinating solvent CH_3CN vs. less coordinating CH_2Cl_2) and phase condi-

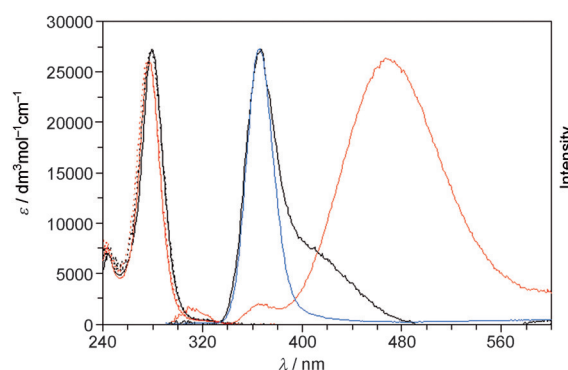
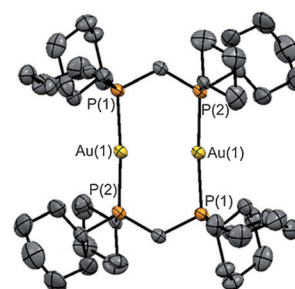


Figure 1. Top: ORTEP drawing of **1**.^[7a] Bottom: Steady-state absorption, normalized emission ($\lambda_{\text{ex}} = 280$ nm), and excitation spectra (---) of **1**·(ClO_4)₂ in degassed CH_3CN (—), CH_2Cl_2 (—), and in the solid-state (—) at room temperature.

[a] Prof. Dr. C. Ma, Dr. W.-P. To, Prof. Dr. C.-M. Che
State Key Laboratory of Synthetic Chemistry
Institute of Molecular Functional Materials
Department of Chemistry, The University of Hong Kong
Pokfulam Road, Hong Kong (P. R. China)
E-mail: cmche@hku.hk

[b] Prof. Dr. C.-M. Che
HKU Shenzhen Institute of Research and Innovation
Shenzhen 518053 (P. R. China)

[c] C. T.-L. Chan, Dr. W.-M. Kwok
Department of Applied Biology and Chemical Technology
The Hong Kong Polytechnic University
Hung Hom, Kowloon, Hong Kong (P. R. China)
E-mail: wm.kwok@polyu.edu.hk

[d] Prof. Dr. C. Ma
School of Chemistry and Environmental Engineering
Shenzhen University, Shenzhen, 518060 (P. R. China)

Supporting information for this article is available on the WWW under <http://dx.doi.org/10.1002/chem.201503045>.

tions (solution vs. solid phase), $1\cdot(\text{ClO}_4)_2$ features characteristic low energy absorption due to the strongly spin and optical allowed metal centred (MC) $\text{Au-Au } 5d\sigma^* \rightarrow 6p\sigma$ transition ($\epsilon_{\text{max}} \sim 2.6\text{--}2.7 \times 10^4 \text{ dm}^3 \text{ mol}^{-1} \text{ cm}^{-1}$). This transition promotes electrons from the anti-bonding $5d_z^2$ to the bonding combination of $6s/6p_z$ orbital (with the Au–Au axis defined as the z axis) leading to enhanced metal–metal interactions and an increase in the Au–Au formal bond order from 0 in the ground state (S_0) to 1 in the ${}^15d\sigma^*6p\sigma$ excited state.^[17,18] Complex $1\cdot(\text{ClO}_4)_2$ in the solid state features an intense near-UV emission with $\lambda_{\text{max}} \sim 370 \text{ nm}$ ($\Phi_e \sim 0.37$). In CH_2Cl_2 , the complex is much less luminescent ($\Phi_e \sim 0.01$) showing still the $\sim 370 \text{ nm}$ emission but with an added weak shoulder at $\sim 420 \text{ nm}$. In contrast, $1\cdot(\text{ClO}_4)_2$ in CH_3CN exhibits emission ($\Phi_e \sim 0.05$) dominated by a distinct broad profile ($\lambda_{\text{max}} \sim 480 \text{ nm}$) along with a very weak band at $\sim 315 \text{ nm}$ and the emission at $\sim 370 \text{ nm}$ has a reduced intensity compared to that in CH_2Cl_2 and in the solid state. The $\sim 480 \text{ nm}$ emission is typical of those reported for analogous bi/multi-nuclear Au^I complexes.^[1c,d,7,8] As depicted also in Figure 1, the luminescence in CH_3CN , CH_2Cl_2 and the solid phase features a similar excitation spectrum that resembles the corresponding low energy absorption. As a result, these seemingly very different emissions must arise due to altered dynamic evolutions of the common $5d\sigma^* \rightarrow 6p\sigma$ excitation. Early studies ascribed the broad visible region emission to the MC triplet state of ${}^35d\sigma^*6p\sigma$ or ${}^35d\delta^*6p\sigma$;^[1,2] more recent work from both experimental and theoretical perspectives showed that the ${}^35d\sigma^*6p\sigma$ is in fact responsible for the $\sim 370 \text{ nm}$ emission, whereas the emission at visible wavelengths is given by a triplet exciplex that is formed from substrate binding of the ${}^35d\sigma^*6p\sigma$ with solvent or/and the counter anion (${}^3\text{SB}$ hereafter).^[7]

To develop $[\text{Au}_2(\text{diphosphine})_2]^{2+}$ as a new photocatalyst for light-induced inner-sphere C–X activation, the issues to be addressed/clarified include the dynamic pathway(s) of the ${}^35d\sigma^*6p\sigma$ state and whether this excited state could be formed with high efficiency and has sufficient lifetime to allow for substrate binding to occur at the open coordination site of Au^I in solution. To address these issues, a comparative time-resolved (TR) study performed with a conjunction of fs TR fluorescence (fs-TRF), transient absorption (fs-TA), ps- and ns-TR emission (TRE) on $1\cdot(\text{ClO}_4)_2$ in the solid state and in solution of CH_3CN and CH_2Cl_2 was undertaken. By monitoring directly temporal evolution of excited-state spectra over a time span from tens of fs to tens of μs after the $5d\sigma^* \rightarrow 6p\sigma$ excitation, this work unveils an ultrafast ${}^15d\sigma^*6p\sigma \rightarrow {}^35d\sigma^*6p\sigma$ intersystem crossing (ISC) and a remarkably rapid rate of the ${}^35d\sigma^*6p\sigma$ to coordinate with solvent in CH_3CN or to perform a redox reac-

tion in CH_2Cl_2 . The ${}^35d\sigma^*6p\sigma$ is highly reactive and events occurring at very early times play a crucial role in accounting for the luminescence and photochemical reactivity of $[\text{Au}_2(\text{diphosphine})_2]^{2+}$ complexes.

Fs-TRF measurement realized based on a time-gating technique (details in the Supporting Information) was done to probe fluorescence as a function of time after excitation (at 280 nm) into the $5d\sigma^*6p\sigma$ state. Figure 2 shows the TRF spec-

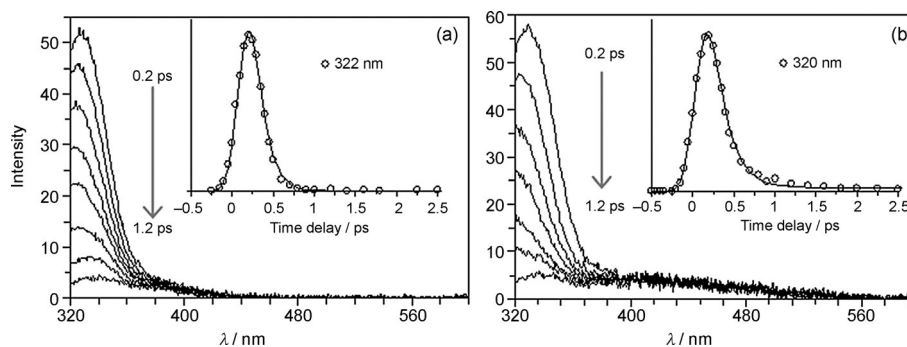


Figure 2. Fs-TRF spectra recorded with 280 nm excitation of $1\cdot(\text{ClO}_4)_2$ in (a) CH_2Cl_2 and (b) CH_3CN . Insets show experimental (\circ) and fitted (—) kinetic decay profiles at denoted fluorescence wavelengths. Arrows indicate temporal evolution of the TRF.

tra recorded with $1\cdot(\text{ClO}_4)_2$ in CH_2Cl_2 and CH_3CN ; the result in the solid state is given in Figure S1 in the Supporting Information. For all the three studied cases, the TRF, which arises from photogenerated ${}^15d\sigma^*6p\sigma$, display a common profile with $\lambda_{\text{max}} \sim 315 \text{ nm}$ and deplete promptly with a $\sim 0.13\text{--}0.18 \text{ ps}$ time constant (insets in Figure 1 and Figure S1, Supporting Information).

The very rapid decay of TRF is indicative of the presence of a highly efficient non-radiative process to deactivate the ${}^15d\sigma^*6p\sigma$. To interrogate the nature of this process, a parallel fs-TA measurement was conducted and the spectra obtained in CH_2Cl_2 and CH_3CN are compared in Figure 3; the corresponding TA time profiles are given in Figure S2 in the Supporting Information. Temporal evolutions of TA in the two solvents are very similar at early times ($< \sim 1 \text{ ps}$) but they differ distinctively at time intervals beyond $\sim 1 \text{ ps}$ after excitation.

In both CH_2Cl_2 and CH_3CN , the TA at initial time (0.2 ps) feature broad absorption with λ_{max} at ~ 355 and 480 nm ; the spectrum evolves with a $\sim 0.14\text{--}0.16 \text{ ps}$ time constant (Figures S2a and S2c, Supporting Information) into a varied profile with $\lambda_{\text{max}} \sim 365 \text{ nm}$ accompanied with an isosbestic point at $\sim 413 \text{ nm}$ (Figure 3a,c). Upon formation, the $\sim 365 \text{ nm}$ TA persists in tens of ps (Figure 3b and Figure S2b, Supporting Information) and decays with a time constant of $\sim 510 \text{ ps}$ (Figure S3, Supporting Information) in CH_2Cl_2 . Unlike this example, the $\sim 365 \text{ nm}$ TA in CH_3CN transforms with a $\sim 4.5 \text{ ps}$ time constant (Figure S2d, Supporting Information) into yet another profile with $\lambda_{\text{max}} \sim 422 \text{ nm}$ with a concomitant pair of isosbestic points at ~ 388 and 527 nm (Figure 3d). The $\sim 422 \text{ nm}$ TA is long-lived with an

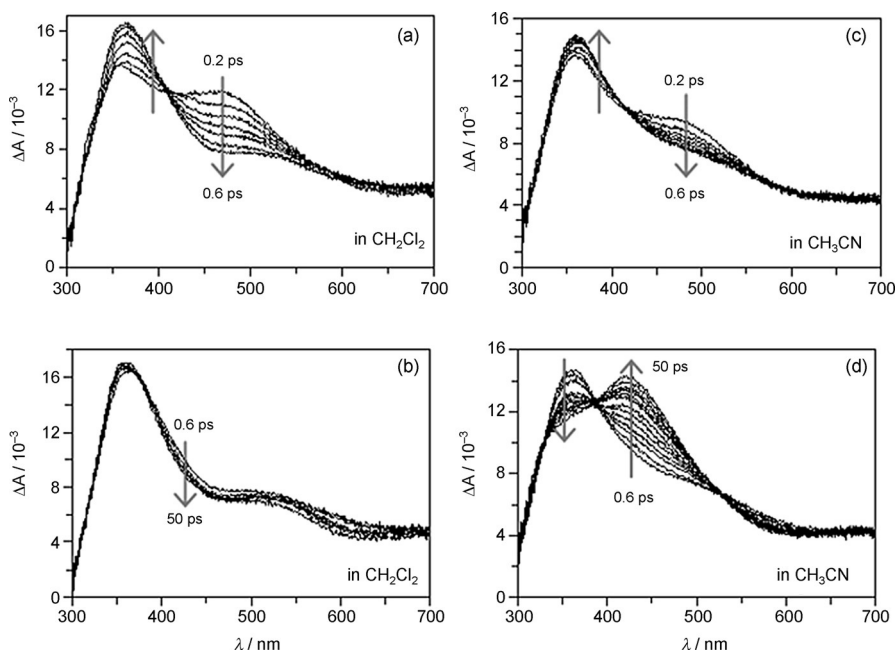


Figure 3. fs-TA spectra recorded for $1\text{-(ClO}_4)_2$ in (a,b) CH_2Cl_2 and (c,d) CH_3CN at early (a,c) and late (b,d) times after 280 nm excitation. Arrows show directions of spectral evolution.

intensity kept unchanged over a timescale up to several ns after the excitation.

The $\sim 0.14\text{--}0.16$ ps time constant of the first-phase TA evolution coincides with the fluorescence decay time observed in the fs-TRF. The initial $\sim 355/480$ nm TA is, therefore, corresponding to absorption ($S_1 \rightarrow S_n$) of the ${}^15d\sigma^*6p\sigma$ (S_1) while the ~ 365 nm (Figure 3a,b) absorption is assigned to an immediate product produced by non-radiative decay of the ${}^15d\sigma^*6p\sigma$. Of note, the ~ 365 nm (in both CH_2Cl_2 and CH_3CN) and ~ 422 nm (in CH_3CN only) species in TA shows no dynamic counterparts in the fs-TRF (Figure 2). Therefore, these species, which are formed in high yield (as suggested by their rapid formation rates), must be very weakly emissive featuring a reduced (by 10-fold or more) radiative rate constant (k_r) when compared to that of the ${}^1d\sigma^*6p\sigma$ (which displays spin-allowed fluorescence emission with $k_r = \sim 2.6 \times 10^8 \text{ s}^{-1}$ according to the Strickler-Berg equation).

To resolve the identities of ~ 365 and ~ 422 nm TA (Figure 3a,b) and their relevance to the steady-state emission in Figure 1, Figure 4 shows TRE spectra and the related decay profiles acquired with $1\text{-(ClO}_4)_2$ in CH_2Cl_2 and CH_3CN , the data in the solid state is depicted in Figure S4 in the Supporting Information. Unlike fs-TRF (Figure 2), which was recorded by using an ultra-short gating duration (~ 100 fs) for the detection of strongly optically allowed emis-

sion, the TRE were produced by employing an adequately prolonged gating time (~ 3 ps in CH_2Cl_2 ; ~ 2 ns in CH_3CN and the solid state) to allow capturing emission from a longer-lived and relatively weakly emissive state (details in the Supporting Information).

The TRE in CH_2Cl_2 (Figure 4a) and in the solid state (Figure S4, Supporting Information) feature similar spectra that are nearly identical to the ~ 370 nm steady-state emission from ${}^35d\sigma^*6p\sigma$;[7] the emission lifetime was measured to be ~ 4.3 μs in the solid state and ~ 510 ps in CH_2Cl_2 . The latter is equivalent to the decay time of ~ 365 nm TA in the same solvent, which indicates a common origin, that is, the ~ 365 nm TA is also from the ${}^35d\sigma^*6p\sigma$ (T_1), corresponding to absorption signature ($T_1 \rightarrow T_n$) of this state. The much shorter lifetime of the ${}^35d\sigma^*6p\sigma$ in CH_2Cl_2 corroborates with the markedly reduced Φ_e in this solvent compared to that in the solid state, revealing the presence of an effective quenching process to the ${}^35d\sigma^*6p\sigma$ (T_1) in CH_2Cl_2 . On the other hand, the TRE in CH_3CN shows spectra resembling the ~ 480 nm steady-state emission due to ${}^3\text{SB}$, the decay of which occurs on a timescale consistent with the ~ 422 nm species in fs-TA. The ~ 422 nm TA can thus be ascribed to the absorption spectrum of the ${}^3\text{SB}$.

The decay dynamics of TRE (in CH_3CN) from tens of ns to several μs was, however, found to be complex with the time profile deviating strongly from singlet exponential and the emission spectrum displaying a subtle but clear redshift from $\lambda_{\text{max}} \sim 480$ nm at 10 ns to $\lambda_{\text{max}} \sim 510$ nm at 5 μs after excitation. A proper fit to the kinetic decay requires a multi-exponential function described by at least three components of ~ 52 ns,

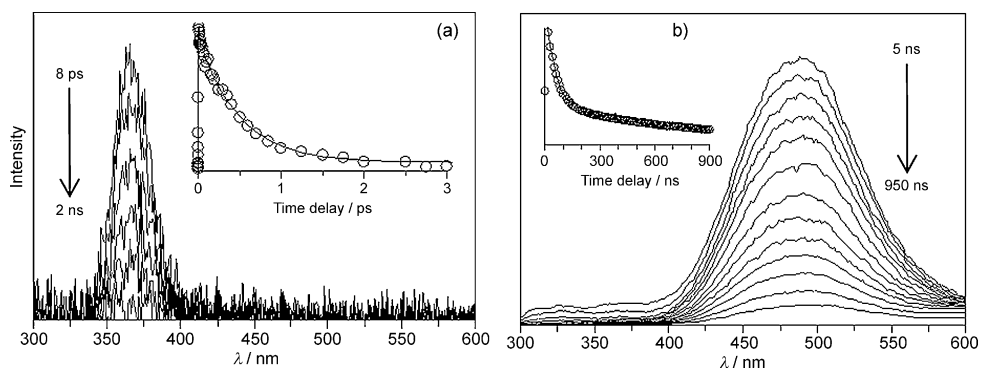
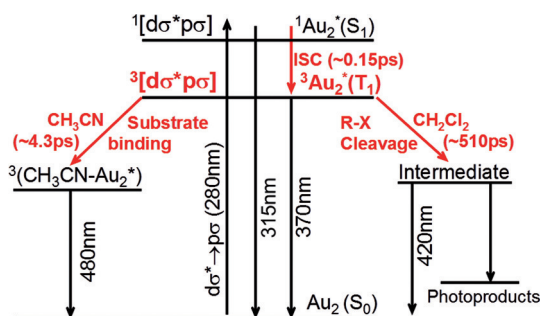


Figure 4. TRE spectra recorded with $1\text{-(ClO}_4)_2$ at various times after 280 nm excitation in (a) CH_2Cl_2 and (b) CH_3CN . Insets show the experimental (○) and fitted (—) decay profile from the corresponding TRE.

	λ_{abs} [nm] ^[a]	λ_{em} [nm] ^[b]	Solid state	τ ^[c] CH_2Cl_2	CH_3CN
$^1d\sigma^*6p\sigma$	355, 480	315	0.18 ps	0.15 ps	0.13 ps
$^3d\sigma^*6p\sigma$	365	370	4.3 μs	510 ps	4.5 ps
^3SB	422	480–510			52 ns, 910 ns, 3.2 μs

[a] Absorption wavelength maximum from fs-TA. [b] Emission wavelength maximum from fs-TRF and ns-TRE. [c] Decay time constant.



Scheme 1. Dynamics and deactivation diagram proposed for $1\text{-(ClO}_4)_2$ in the solid state (middle), CH_3CN (left) and CH_2Cl_2 (right).

~ 910 ns and $3.2 \mu\text{s}$ time constant with a fraction contribution of ~ 79.6 , ~ 19.9 and $\sim 0.5\%$, respectively.

Taking together the key spectral features and the direct dynamic interplays between them (Table 1), the following excited-state cascade for the environmental dependent emission of $1\text{-(ClO}_4)_2$ is constructed (Scheme 1). Upon excitation, the $^1d\sigma^*6p\sigma$ (S_1) which features $\lambda_{\text{max}} \sim 315$ nm emission, depletes by ISC with a ~ 0.15 ps time constant to the $^3d\sigma^*6p\sigma$ (T_1). This occurs as a common process invariant with the phase condition and solvent properties. The $^3d\sigma^*6p\sigma$ (T_1) after formation, decays with lifetime of ~ 510 ps in CH_2Cl_2 and $\sim 4.3 \mu\text{s}$ in the solid phase producing the ~ 370 nm emission. In CH_3CN , the $^3d\sigma^*6p\sigma$ (T_1) transforms with a ~ 4.5 ps time constant through substrate binding to yield ^3SB , which gives the ~ 480 nm emission exhibiting multi-exponential decay with 52 ns/910 ns/3.2 μs time constants. The ~ 0.15 and 4.3 ps rates of ISC (τ_{ISC}) and substrate binding are very rapid, exceeding greatly those of the radiative decay or other likely deactivation process. This implies close to unitary quantum efficiency for both the processes, when considering their non-radiative nature is responsible for the minute ~ 315 nm fluorescence in the steady-state emission in all three examined conditions and the minimal ~ 370 nm $^3d\sigma^*6p\sigma$ (T_1) phosphorescence in CH_3CN . Moreover, that the ^3SB is involved only in CH_3CN but not in CH_2Cl_2 presents compelling evidence that the ^3SB is brought about by $^3d\sigma^*6p\sigma$ binding to CH_3CN solvent, rather than ClO_4^- counter anion. This assignment is corroborated by the ~ 4.5 ps binding rate, which is much faster than could be expected for binding with the counter anion. The latter is a process limited by the dynamics of diffusion, which occurs typically in the timescale from several to tens of ns under the conditions of solvent and sample concentration ($\sim 10^{-4}$ M) used in this study.^[19]

ISC in ultrafast (tens of fs to several ps) timescale has been documented for a number of 1st, 2nd and 3rd row metal complexes containing metals such as Fe^{II} ,^[20] Ru^{II} ,^[21] Re^{I} ,^[22] Pt^{II} ^[23] or (mononuclear) Au^{I} .^[24] The work here is, however, the first direct study on ISC for the type of $d^{10}\text{-}d^{10}$ bi- Au^{I} (Au_2^{I} for short) complexes. The ~ 150 fs ISC ($^15d\sigma^*6p\sigma \rightarrow ^35d\sigma^*6p\sigma$) of **1** appears not surprisingly in regard to the large spin-orbital coupling (SOC) constant (ξ) of gold and the heavy atom effect in promoting the ISC. The result is, however, significant when noting the relatively slow ISC reported for the counterpart states in $d^8\text{-}d^8$ analogues such as $[\text{Rh}_2\text{L}_4]^{2+}$ (denoted Rh_2^{I} , L = 2,5-dimethyl-2,5-diisocyanohexane, $\tau_{\text{ISC}} = \sim 820$ ps)^[25] and the classic $[\text{Pt}_2(\text{P}_2\text{O}_5\text{H}_2)_4]^{4-}$ (denoted Pt_2^{II} , $\tau_{\text{ISC}} = \sim 15\text{-}29$ ps).^[26] Indeed, there is increasing evidence that the ISC rate of metal complex is not governed solely by SOC strength of the metal.^[24-28] The slow ISC rate of Pt_2^{II} was ascribed to symmetry forbidden (in D_{4h}) for the SOC between $^1,^35d\sigma^*6p\sigma$, a large singlet-triplet energy splitting ($\Delta E = \sim 5000 \text{ cm}^{-1}$ in Pt_2^{II}), and a lack of mediating triplet state between the $^1,^35d\sigma^*6p\sigma$. The tens of ps ISC rate of Pt_2^{II} was proposed in a recent study to occur due to symmetry lowering induced by structure distortion in the excited state from the S_0 .^[26] The $^1,^35d\sigma^*6p\sigma$ of Au_2^{I} have an electronic nature and energy gap ($\Delta E = \sim 4700 \text{ cm}^{-1}$ according to the $\sim 315/370$ nm emission for $^1d\sigma^*6p\sigma/^3d\sigma^*6p\sigma$, Figures 2 and 4 and Table 1) similar to that of the $^1,^35d\sigma^*6p\sigma$ of Pt_2^{II} . One major difference in the $^1,^35d\sigma^*6p\sigma$ between Au_2^{I} and Pt_2^{II} is that, as a result of the linear 2-coordination in Au^{I} versus the planar 4-coordination in Pt^{II} , the Au_2^{I} features symmetry (D_{2h}) lower than that of Pt_2^{II} . We conceive that, apart from the somewhat more favourable SOC strength ($\xi = \sim 5000/4000 \text{ cm}^{-1}$ for Au/Pt), the low symmetry could be among the main factors for the ultrafast ISC (by $> 10^2$ -fold faster than τ_{ISC} of Pt_2^{II}) exhibited by the Au_2^{I} complex **1**.

The very rapid rate (~ 4.3 ps) of $^3d\sigma^*6p\sigma \rightarrow ^3\text{SB}$ conversion testifies that the $^3d\sigma^*6p\sigma$ state has an unprecedentedly strong proclivity towards increasing coordination number at the Au^{I} centres. This is associated with the open coordination framework of the Au^{I} centres in **1**. That the binding occurs in such a rapid timescale is remarkable. It is worth noting that the binding to CH_3CN , albeit very fast, is slow compared to the reorientation solvation dynamics (~ 0.24 ps) of CH_3CN .^[29] This implies the presence of a certain free-energy barrier along the path from precursor $^3d\sigma^*6p\sigma$ to the ^3SB product. Most likely, this is due to an involvement of substantial entropy of activation that is caused by the steric hindrance imposed by the bulky phosphine groups and to reposition solvent molecules to the required orientation for the development of the binding through the coordinating end (cyano group) of CH_3CN to the Au^{I} centre. Moreover, the multi-exponential decay and the concurrent redshift of the ^3SB emission are evidence indicating the complex composition of the ^3SB , which we ascribe to stem from the ^3SB being made up of an ensemble of species that have the Au^{I} centres coordinated to a varied number of CH_3CN molecules. These species, depending on the coordination number, might be energetically stabilized to a varied degree (with respect to the $^3d\sigma^*6p\sigma$) and have a different tendency towards de-solvation into solvent molecules and the S_0 of

1 (non-radiative decay of the ^3SB). The one stabilized to a greater degree (therefore emission at longer wavelength) is less prone to de-solvation and thus has a longer lifetime. This explains the result that the longer wavelength ^3SB emission features slower decay.

The 510 ps dynamic quenching of ~ 370 nm emission in CH_2Cl_2 provides compelling evidence for strong reactivity of the $^3\text{d}\sigma^*6\text{p}\sigma$ state. It was noted that $[\text{Au}_2(\text{dppm})_2]^{2+}$ complex (dppm = bis(diphenylphosphino)methane) is photochemically reactive towards alkyl halide (R–X) leading to the R–X bond cleavage and formation of $[\text{Au}_2(\text{dppm})\text{X}_2]$ upon light excitation.^[1b,c,d] On the basis of this, we tentatively attribute the quenching of ~ 370 nm emission in CH_2Cl_2 to arising due to an inner-sphere reaction between the $^3\text{d}\sigma^*6\text{p}\sigma$ and surrounding CH_2Cl_2 molecule(s). Associated with this, we noticed observation in the fs-TA measurement of the $^3\text{d}\sigma^*6\text{p}\sigma$ spectrum evolving into an alternative profile (Figure S3a, Supporting Information) which is attributable to a transient species formed intimately by the quenching reaction and being involved in the dynamic processes that yield the final photoproducts. The entire reaction mechanism, which is complex and presumably proceeding through multiple steps over extensive timescales, was, however, not assessed owing to the limited detection time window ($< \sim 6$ ns) of the current fs-TA measurement. Of note, the 510 ps quenching rate is rather rapid, implying that the related reaction, either by a mechanism of atom or electron transfer, could be highly effective. We noted that steady-state photolysis of $[\text{Au}_2(\text{dcpm})_2]^{2+}$ in CD_2Cl_2 gave $[\text{Au}_2(\text{dcpm})\text{Cl}_2]$ and similar photochemistry was observed with $[\text{Au}_2(\text{dppm})_2]^{2+}$.^[1b] The ^{31}P NMR spectrum of the solution (Figure S5, Supporting Information) showed that, after irradiation with light ($\lambda > 260$ nm, 300 W Xenon arc lamp) for 45 min, the ^{31}P signal of $[\text{Au}_2(\text{dcpm})\text{Cl}_2]$ at 46.16 ppm emerged as the major new species; both the free dcpm ligand ($\delta = -10.3$ ppm) and its oxide ($\delta = 48.5$ ppm) were not observed (the ^{31}P NMR spectroscopic data of $[\text{Au}_2(\text{dcpm})\text{Cl}_2]$ was also obtained by independent preparation of this complex in this study). It is proposed that the $^3\text{d}\sigma^*6\text{p}\sigma$ excited state of **1** initially abstracts chloride from CH_2Cl_2 to give $[\text{Au}_2(\text{dcpm})_2\text{Cl}]^{2+}$. The as-formed $[\text{Au}_2(\text{dcpm})_2\text{Cl}]^{2+}$ intermediate is unstable, and undergoes further complex reactions to give $[\text{Au}_2(\text{dcpm})\text{Cl}_2]$ as the observed photoproduct. The mechanism for conversion of $[\text{Au}_2(\text{dcpm})_2\text{Cl}]^{2+}$ to give $[\text{Au}_2(\text{dcpm})\text{Cl}_2]$ is complex and further study is necessary. Given the reactivity of the $^3\text{d}\sigma^*6\text{p}\sigma$ excited state of **1**, we performed the photochemical reactions of **1**·(OTf)₂ with secondary alcohols and cyclohexene with an objective to observe light-induced C–H bond cleavage (details given in the Supporting Information). The triflate salt of **1** was used because of better solubility. Upon irradiation of **1** in the presence of isopropyl alcohol at $\lambda > 260$ nm with a 300 W Xenon arc lamp, production of hydrogen, acetone and pinacol was observed with turnovers of 2.5, 6.2 and 2.6 respectively. Similar photolysis of **1** in the presence of cyclohexanol gave cyclohexanone with 19 turnovers. For the photochemical reaction with cyclohexene, 15 turnovers of 1,1'-bi(cyclohex-2-ene), which is the coupling product of two allylic radicals of cyclohexene, have been furnished. These findings are similar to the

photochemical C–X and C–H bond cleavage reactions of $[\text{Pt}_2(\text{P}_2\text{O}_5\text{H}_2)_4]^{4-}$.^[9b] The lower efficiency could be due to the shorter lifetime of the $^3\text{d}\sigma^*6\text{p}\sigma$ excited state of **1** in solution.

In summary, we report the first fs time-resolved spectroscopic characterization for excited states of a prototype Au^1_2 complex **1**, and the first direct comparison of excited state dynamics in inert conditions (the solid state) versus in solvents (CH_3CN and CH_2Cl_2) to unravel early time events that are involved in accounting for the intriguing environmentally dependent photoluminescence and the varied photochemical behaviour of Au^1_2 complexes. The $^3\text{d}\sigma^*6\text{p}\sigma$ state, which is formed, regardless of the environmental conditions, with a ~ 0.15 ps time constant through ISC from the initially excited $^1\text{d}\sigma^*6\text{p}\sigma$ state, is viable and highly reactive, being at the same time a powerful reagent for photochemical reactions and with astonishingly strong propensity toward increasing the coordination number at the Au^1 centres. These findings provide a benchmark example for understanding the photophysics and photochemistry of di/multi-nuclear Au^1 complexes.

Acknowledgements

We thank the National Natural Science Foundation of China (No. 21473114), the National Key Basic Research Program of China (2013CB834802), the Area of Excellence Program (AoE/P-03/08), the Research Grants Council of Hong Kong (PolyU/5009/11P and PolyU/5009/13P), and the Hong Kong Polytechnic University (G-YBAU and G-YM51) for the financial support.

Keywords: femtosecond time-resolved fluorescence · gold · photocleavage · substrate binding · transient absorption

- [1] a) C.-M. Che, S.-W. Lai, *Coord. Chem. Rev.* **2005**, *249*, 1296–1309; b) D. Li, C.-M. Che, H.-L. Kwong, V. W.-W. Yam, *J. Chem. Soc. Dalton Trans.* **1992**, 3325–3329; c) C.-M. Che, H.-L. Kwong, V. W.-W. Yam, K.-C. Cho, *J. Chem. Soc. Chem. Commun.* **1989**, *13*, 885–886; d) C.-M. Che, H.-L. Kwong, C.-K. Poon, V. W.-W. Yam, *J. Chem. Soc. Dalton Trans.* **1990**, *11*, 3215–3219.
- [2] a) V. W.-W. Yam, E. C.-C. Cheng, *Top. Curr. Chem.* **2007**, *281*, 269–309; b) V. W.-W. Yam, E. C.-C. Cheng, *Chem. Soc. Rev.* **2008**, *37*, 1806–1813.
- [3] R. F. Ziolo, S. Lipton, Z. Dori, *J. Chem. Soc. D* **1970**, 1124–1125.
- [4] M. J. Katz, K. Sakai, D. B. Leznoff, *Chem. Soc. Rev.* **2008**, *37*, 1884–1895.
- [5] a) P. Pyykkö, F. Mendizabal, *Inorg. Chem.* **1998**, *37*, 3018–3025; b) P. Pyykkö, Y. Zhao, *Angew. Chem. Int. Ed. Engl.* **1991**, *30*, 604–605; *Angew. Chem.* **1991**, *103*, 622–623.
- [6] a) Y. Takemura, H. Takenaka, T. Nakajima, T. Tanase, *Angew. Chem. Int. Ed.* **2009**, *48*, 2157–2161; *Angew. Chem.* **2009**, *121*, 2191–2195; b) M. A. Rawashdeh-Omary, M. A. Omary, H. H. Patterson, J. P. Fackler, *J. Am. Chem. Soc.* **2001**, *123*, 11237–11247.
- [7] a) W.-F. Fu, K.-C. Chan, V. M. Miskowski, C.-M. Che, *Angew. Chem. Int. Ed.* **1999**, *38*, 2783–2785; *Angew. Chem.* **1999**, *111*, 2953–2955; b) W.-F. Fu, K.-C. Chan, K.-K. Cheung, C.-M. Che, *Chem. Eur. J.* **2001**, *7*, 4656–4664.
- [8] G. S. M. Tong, S. C. F. Kui, H.-Y. Chao, N. Zhu, C.-M. Che, *Chem. Eur. J.* **2009**, *15*, 10777–10789.
- [9] a) D. C. Smith, H. B. Gray, *Coord. Chem. Rev.* **1990**, *100*, 169–181; b) D. M. Roundhill, H. B. Gray, C.-M. Che, *Acc. Chem. Res.* **1989**, *22*, 55–61.
- [10] A. E. Stiegman, S. F. Rice, H. B. Gray, V. M. Miskowski, *Inorg. Chem.* **1987**, *26*, 1112–1116.
- [11] V. W.-W. Yam, C.-K. Li, C.-L. Chan, *Angew. Chem. Int. Ed.* **1998**, *37*, 2857–2859; *Angew. Chem.* **1998**, *110*, 3041–3044.
- [12] M. A. Mansour, W. B. Connick, R. J. Lachicotte, H. J. Gysling, R. Eisenberg, *J. Am. Chem. Soc.* **1998**, *120*, 1329–1330.

- [13] Y. Ma, C.-M. Che, H.-Y. Chao, X. Zhou, W.-H. Chan, J. Shen, *Adv. Mater.* **1999**, *11*, 852–857.
- [14] R. L. White-Morris, M. M. Olmstead, A. L. Balch, *J. Am. Chem. Soc.* **2003**, *125*, 1033–1040.
- [15] a) G. Revol, T. McCallum, M. Morin, F. Gagosz, L. Barriault, *Angew. Chem. Int. Ed.* **2013**, *52*, 13342–13345; *Angew. Chem.* **2013**, *125*, 13584–13587; b) T. McCallum, E. Slavko, M. Morin, L. Barriault, *Eur. J. Org. Chem.* **2015**, 81–85.
- [16] J. Xie, S. Shi, T. Zhang, N. Mehrkens, M. Rudolph, A. S. K. Hashmi, *Angew. Chem. Int. Ed.* **2015**, *54*, 6046–6050; *Angew. Chem.* **2015**, *127*, 6144–6148.
- [17] K. H. Leung, D. L. Phillips, M.-C. Tse, C.-M. Che, V. M. Miskowski, *J. Am. Chem. Soc.* **1999**, *121*, 4799–4803.
- [18] a) H.-X. Zhang, C.-M. Che, *Chem. Eur. J.* **2001**, *7*, 4887–4893; b) Q.-J. Pan, H.-X. Zhang, *J. Phys. Chem. A* **2004**, *108*, 3650–3661.
- [19] N. J. Turro, *Modern Molecular Photochemistry*; (University Science Book) Mill Valley, CA, **1991**.
- [20] W. Gawelda, A. Cannizzo, V.-T. Pham, F. van Mourik, C. Bressler, M. Chergui, *J. Am. Chem. Soc.* **2007**, *129*, 8199–8206.
- [21] a) N. H. Damrauer, G. Cerullo, A. Yeh, T. R. Boussie, C. V. Shank, J. K. McCusker, *Science* **1997**, *275*, 54–57; b) A. T. Yeh, C. V. Shank, J. K. McCusker, *Science* **2000**, *289*, 935–938.
- [22] A. Cannizzo, A. M. Blanco-Rodríguez, A. E. Nahhas, J. Šebera, S. Zálíš, A. Vlček Jr., M. Chergui, *J. Am. Chem. Soc.* **2008**, *130*, 8967–8974.
- [23] a) C. E. Whittle, J. A. Weinstein, M. W. George, K. S. Schanze, *Inorg. Chem.* **2001**, *40*, 4053–4062; b) G. Ramakrishna, T. Goodson III, J. E. Rogers-Haley, T. M. Cooper, D. G. McLean, A. Urbas, *J. Phys. Chem. C* **2009**, *113*, 1060–1066.
- [24] a) W. Lu, W.-M. Kwok, C. Ma, C. T.-L. Chan, M.-X. Zhu, C.-M. Che, *J. Am. Chem. Soc.* **2011**, *133*, 14120–14135; b) C. Ma, C. T.-L. Chan, W.-M. Kwok, C. M. Che, *Chem. Sci.* **2012**, *3*, 1883–1892.
- [25] a) J. R. Winkler, J. L. Marshall, T. L. Netzel, H. B. Gray, *J. Am. Chem. Soc.* **1986**, *108*, 2263–2266; b) V. M. Miskowski, G. L. Nobinger, D. S. Kliger, G. S. Hammond, N. S. Lewis, K. R. Mann, H. B. Gray, *J. Am. Chem. Soc.* **1978**, *100*, 485–488.
- [26] R. M. van der Veen, A. Cannizzo, F. van Mourik, A. Vlček Jr., M. Chergui, *J. Am. Chem. Soc.* **2011**, *133*, 305–315.
- [27] A. Steffen, M. G. Tay, A. S. Batsanov, J. A. K. Howard, A. Beeby, K. Q. Vuong, X.-Z. Sun, M. W. George, T. B. Marder, *Angew. Chem. Int. Ed.* **2010**, *49*, 2349–2353; *Angew. Chem.* **2010**, *122*, 2399–2403.
- [28] G. S. M. Tong, P. K. Chow, C.-M. Che, *Angew. Chem. Int. Ed.* **2010**, *49*, 9206–9209; *Angew. Chem.* **2010**, *122*, 9392–9395.
- [29] M. L. Horng, J. A. Gardecki, A. Papazyan, M. Maroncelli, *J. Phys. Chem.* **1995**, *99*, 17311–17337.

Received: August 3, 2015

Published online on September 4, 2015